Article

Potential of hydroxybenzoic acids from *Graptopetalum paraguayense* for inhibiting of herpes simplex virus DNA polymerase – metabolome profiling, molecular docking and quantum-chemical analysis

Nadezhda Todorova[1], Miroslav Rangelov[2], Ivayla Dincheva[3], Ilian Badjakov[3], Venelin Enchev[4],

Nadezhda Markova[2]*

[1] Institute of Biodiversity and Ecosystem Research, Bulgarian Academy of Sciences, 1113 Sofia, Bulgaria, nadeshda@abv.bg
[2] Institute of Organic Chemistry with Centre of Phytochemistry, Bulgarian Academy of Sciences, 1113 Sofia, Bulgaria, nadya@orgchm.bas.bg , marangelov@gmail.com
[3] Department of Agrobiotechnologies, Agrobioinstitute, Agricultural Academy, 1164 Sofia, Bulgaria, ivadincheva@yahoo.com , ibadjakov@gmail.com
[4] Institute of General and Inorganic Chemistry, Bulgarian Academy of Sciences, 1113 Sofia, Bulgaria, venelin@srv.igic.bas.bg
* Correspondence: nadya@orgchm.bas.bg Institute of Organic Chemistry with Centre of Phytochemistry, Bulgarian Academy of Sciences, "Acad. G. Bonchev" str., bldg. 9, 1113 Sofia, Bulgaria

Abstract: According to our previous investigation the total methanol extract from *Graptopetalum paraguayense* E. Walther demonstrates a significant inhibitory effect on HSV-1. To clarify what causes this inhibitory activity on HSV-1, a metabolic profile of the plant was performed. Three main fractions: non-polar substances, polar metabolites and phenolic compounds were obtained and GC-MS analysis was carried out. Since it is well known that phenolic compounds show a significant anti-herpes effect and that viral DNA polymerase (DNApol) appears to play a key role in HSV virus replication, we present a docking and quantum-chemical analysis of the binding of these compounds to viral DNApol amino acids. Fourteen different phenolic acids found by GS/MS analyses, were used in molecular docking simulations. According to the interaction energies of all fourteen ligands in the DNApol pockets based on docking results, DFT calculations were performed on the five optimally interacting with the receptor acids. It was found that hydroxybenzoic acids from phenolic fraction of *Graptopetalum paraguayense* E. Walther show a good binding affinity to the amino acids from the active site of the HSV DNApol, but significantly lower than that of acyclovir. The mode of action on virus replication of acyclovir (by DNApol) is different from that of the plant phenolic acids one, probably.

Keywords: *Graptopetalum paraguayense* E. Walter, anti-HSV activities, hydroxybenzoic (phenolic) acids, molecular docking, DFT.

1. Introduction

Herpes simplex virus types 1 and 2 (HSV-1 and HSV-2) are members of the *Herpesviridae* family and are among the most common human pathogens, infecting about 90% of the world population [1]. Generally speaking, the main treatments available include several selective drugs that are classified as virucidal, immunomodulators, and chemotherapeutic agents. Common therapies for herpes infections employ nucleoside analogs, such as acyclovir, and target the viral DNA polymerase (DNApol), essential for viral DNA replication. However, the widespread use of such drugs has led to undesirable side effects and drug-resistant strains [2]. A better understanding of the

herpes virus replication will help the development of new safe and effective broad-spectrum anti-herpetic drugs that fill an unmet need.

When searching for potent bioactive compounds, it is especially important to understand the nature of the interaction between biological macromolecules (enzymes, receptors) and small ligands (inhibitors, drugs). Theoretical chemistry can be used for the prediction of chemical structures and reactions, which would support biological testing, save time and resources. A promising way is to combine the complete three-dimensional structure of the biomacromolecule-ligand complex with theoretical energy calculations [3]. A very important methodology for elucidating the reaction mechanisms and other properties of enzymes is the so-called quantum chemical cluster: a small part of the enzyme around the active site is treated with relatively accurate quantum chemical methods [4]. Quantum-chemical calculations, most commonly density functional theory (DFT), are increasingly crucial in computational enzymology.

The first studies on the antiviral activity of plant extracts were carried out in 1995-1996, and since then, researchers have made great strides in finding new plant sources of antiviral compounds. Plants are a rich and growing source of natural target molecules with different chemical structures that exhibit antiviral activity. Bioactive compounds are an important component in various extracts with potential anti-HSV activities. Crude extracts obtained from plants by various extraction methods have shown a wide spectrum of antiviral activity, including anti-HSV activity. A decisive factor for the ultimate success of the study of bioactive plant ingredients is the correct selection of plant materials and the appropriate process of extraction and purification of the active compounds. The main phytochemical substances that possess antiviral effects against HSV-1 and HSV-2 could be included in the following groups: alkaloids and nitrogenated compounds, coumarins, flavonoids, lignans, miscellaneous compounds, monoterpenoids, diterpenoids and sesquiterpenoids, phenolic acids, phenylpropanoids, quinones, tannins, thiophenes, triterpenoids and polyacetylenes [5-7]. Phenolic compounds attract great interest due to their antioxidant activity and beneficial effects on human health [8]. Results from preliminary antiviral plate assay of the green solvent (hydro-ethanolic) shoot extract of *Limonium densiflorum* showed that gallic acid and epigallocatechin gallate have strong activity, while pinoresinol and *N-trans*-ferulolyl tyramine have moderate activity [9]. It was found that phenolic compounds from acetonic and methanolic extract of apple pomace inhibit both HSV-1 and HSV-2 replication in Vero cells by more than 50%, at non-cytotoxic concentrations [10].

Viral replication is not the only therapeutic goal studied, as several in vitro studies have shown that many plant extracts (eg aqueous root and bark extract of *Rhus aromatica* L. [11] as well as aqueous and hydroalcoholic extracts of propolis [12]) and their isolated compounds can inhibit the penetration of a virus. The authors attribute the anti-herpetic activity to the interference of the extracts with the viral envelope structures required for adsorption. Phenyl carboxylic acids, as well as polyphenols, have been identified as responsible compounds, although the synergistic activity of the plant complex has been suggested.

Graptopetalum paraguayense E. Walther (GP) is a species of succulent plant that belongs to the jade family *Crassulaceae*, originating from Tamaulipas, Mexico. In Taiwan, *Graptopetalum paraguayense* is a medicinal plant that is considered a vegetable with health benefits. As early as ancient China GP was traditionally used to treat a number of diseases: modulating blood pressure, relieving liver disease, relieving pain and infections, detoxification. Reported biological effects of GP include tyrosinase inhibition [13], antioxidants [14], regulation of hypertension [15, 16], hepatoprotective effect [17, 18], antitumor activity [19], anti-inflammatory [20] and Alzheimer's disease therapy [21]. There are no data in the literature on the antiviral activity (including anti-herpes activity) of GP. Recently we found that the total methanol extract from the plant demonstrates a significant inhibitory effect on HSV-1 [22]. Therefore, it is important to investigate the metabolic profile of the plant and which metabolites are responsible for

this activity. Since virus-encoded DNA polymerase appears to be a key feature in the replication of large DNA viruses such as HSV, we present metabolome analysis of the plant *Graptopetalum paraguayense* E. Walther as well as theoretical investigations on the binding expedient of the compounds from phenolic fraction to viral DNA polymerase amino acids.

2. Results and Discussion

In our pilot study [22] on the anti-herpes activity of *Graptopetalum paraguayense* E. Walther (Figure 1), we showed that the total GP methanol extract demonstrated a significant inhibitory effect on HSV-1 (97.5% cell protection), compared to ACV (with total protection of the cells 100%). The in vitro cytotoxicity assays of the GP extract indicate that it is characterized by a high cell tolerable concentration range. The results showed that the GP extract could be administrated in a concentration range (MNC and lower) that avoids significant cell damage. The present study aims to further clarify both the organic composition of the plant and the mechanism of action of its main phytochemical components.

Figure 1. *Graptopetalum paraguayense* E. Walther.

The GC-MS analysis of the polar fraction enables qualitative and quantitative determination of *Graptopetalum paraguayense* E. Walther components present in the studied sample. A total of 33 compounds belonging to different chemical classes, mainly amino and organic acids, sugar alcohols, mono- and dicarbohydrates were established (Table 1S). The predominant components in the essential amino acid class were leucine (92.04 μg/g DW), phenylalanine (82.72 μg/g DW) and isoleucine (80.74 μg/g DW), whereas in the non-essential amino acids class – tyrosine (37.75 μg/g DW), glycine (34.89 μg/g DW) and proline (33.28 μg/g DW), respectively. The major constituents in class of organic and inorganic acids were malic (1830.54 μg/g DW), citric (110.94 μg/g DW), and phosphoric acids (23.40 μg/g DW). The class of sugar alcohols was characterized by large amount of glycerol (329.58 μg/g DW) and myo-inositol (37.59 μg/g DW). The main components in the class of monocarbohydrates were mannose (1335.38 μg/g DW) and sedoheptulose (803.77 μg/g DW), whereas in the class of dicarbohydrates - sucrose (473.52 μg/g DW).

The amount of phenolic components was 1701.50 μg/g DW (Table 1). The major components identified in this fraction were 1,8-dihydroxyanthraquinone (426.83 μg/g DW), followed by syringic acid (291.36 μg/g DW), *trans*-ferulic acid (218.97 μg/g DW), gallic acid (183.27 μg/g DW), and *p*-coumaric acid (147.80 μg/g DW), which represent 2/3 of the total phenolic compounds.

The main saturated fatty acids were palmitic (432.87 μg/g DW), stearic (122.24 μg/g DW) and behenic (119.56 μg/g DW) acids (Table 2S). Linolenic (2842.50 μg/g DW), linoleic (2522.25 μg/g DW) and oleic (459.56 μg/g DW) acids - 84% from the total lipid compounds.

Overall, *β*-amyrin (2080.86 μg/g DW), *β*-sitosterol (2010.41 μg/g DW), and *α*-tocopherol (1447.18 μg/g DW) were the predominant compounds in the fraction of sterols, terpenoids, and tocopherols (Table 3S).

Table 1. Phenolic components fraction from *G. Paraguayense* determined by GC-MS analysis

#	Name	RT	RI_{lit}	RI_{calc}	µg/g DW
1	Salicylic acid (2TMS)	8.01	1510.2	1510.3	41.57
2	*m*-Hydroxybenzoic acid (2TMS)	8.51	1576.9	1577.0	24.68
3	4-Hydroxyphenylethanol (2TMS)	8.58	1580.6	1580.7	18.35
4	*p*-Hydroxybenzoic acid (2TMS)	9.19	1640.3	1640.4	20.32
5	*p*-Hydroxyphenylacetic acid (2TMS)	9.34	1665.8	1665.9	32.98
6	Phloretic acid (2TMS)	10.89	1763.2	1763.3	58.94
7	Vanillic acid (2TMS)	11.02	1776.0	1776.3	80.32
8	Gentisic acid (3TMS)	11.15	1788.8	1788.9	70.59
9	Protocatechuic acid (3TMS)	11.77	1813.3	1813.4	85.50
10	Syringic acid (2TMS)	12.92	1911.3	1911.4	291.36
11	*p*-Coumaric acid (2TMS)	13.48	1946.9	1947.0	147.80
12	Gallic acid (4TMS)	13.92	1969.0	1969.1	183.27
13	*trans*-Ferulic acid (2TMS)	15.90	2103.0	2103.1	218.97
14	1,8-Dihydroxyanthraquinone	16.25	2125.5	2125.6	426.84
	Total phenolic compounds				1701.50

DW - dried weight, **RT** - retention time, **RI** - Kovàts retention indices, **TMS** - trimethylsilyl derivatives

Fourteen different phenolic acids such as gallic, trans-ferulic, syringic acids, and others found by GS-MS analyses (Table 1) were used in molecular docking simulations. All docked structures were sorted according to their binding energy and the five best ligands according to ligand-pocket interactions were selected: trans-ferulic, gallic, syringic, vanillic and gentisic acids, as well as acyclovir triphosphate for comparison. *Trans*-Ferulic acid, acyclovir triphosphate and their vicinity after docking procedure is shown in Figures 2 and 3 as an example. These five acids have optimal interactions with the receptor and were used in further DFT calculations. As can be seen from the interaction maps in Figures 3 and 4, the main interaction energy terms are hydrogen bond interactions and ionic ones.

To clarify the affinity of trans-ferulic (*t*FA), gentisic (GntA), vanillic (VA), syringic (SA) and gallic acids (GA) (Figure 5) conjugation to amino acids (AA) in DNA polymerase (Figure 6), quantum-chemical calculations at B3LYP/6-31+G(d,p) level were performed based on molecular docking results. We started by modeling hydrogen-bonded complexes between the hydroxybenzoic acids, amino acids and two water molecules (Fig. 7). Thus, the complexes constructed show non-covalent interactions only qualitatively in the enzyme center, but could nevertheless provide indicative information on the inhibitory activity of phenolic acids from GP. The surroundings in the active enzyme pocket of phenolic acids (PA) were simulated as follows: *trans*-Ferulic acid interacts with one molecule of protonated tyrosine (pTyr), two molecules lysine (Lys) and
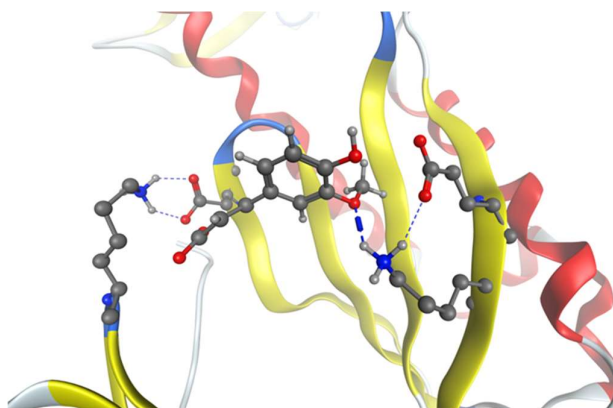
Figure 2. Phenolic (trans-ferulic) acid and its vicinity after docking procedure. The amino acid residues of HSV-1 DNA polymerase active site, mostly involved in interaction with ligands, are represented as follows: Lis928 is basic amino acid right from the ligand, Glu 927 is above it, basic amino acid on the left is Lis 939 and Asp 886 is in its right.
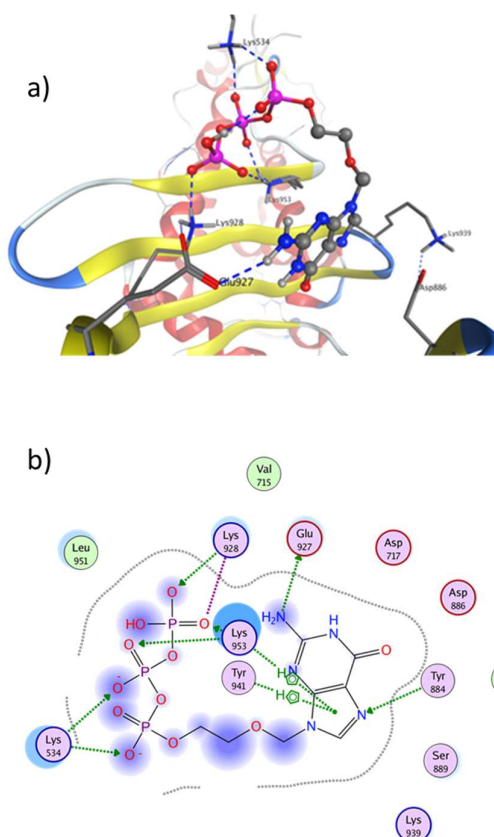

Figure 3. Acyclovir triphosphate and its vicinity in the DNA polymerase pocket after docking procedure: a) 3D plane of view and b) 2D plane of view. The interactions of the ligand in the active site cavity are represented as follows: the proximity contour is depicted with a black dotted line; solvent accessibility, as blue clouds around atoms or blue shadows around amino acid residues; polar amino acids are displayed with pink, while the lipophilic ones are in green. Basic amino acids are outlined with blue and the acidic - with red. Hydrogen bond interactions are depicted with dotted arrows, while the ionic ones are depicted with dotted lines.

two water molecules (*t*Fa-Lys-pTyr-Lys-2H$_2$O); GntA binds by hydrogen bonds to protonated arginine (pArg), glutamic acid (Glu) and two water molecules (GntA-Glu-

pArg-2H$_2$O); vanillic acid conjugates with protonated lysine (pLys), aspartic acid (Asp) and two water molecules (VA-pLys-Asp-2H$_2$O); the binding of SA to pTyr and two water molecules leads to the formation of the hydrogen-bounded complex SA-pTyr-2H$_2$O; gallic acid interacts with pLys, Asp and two water molecules to form GA-Lys-Asp-2H$_2$O complex.
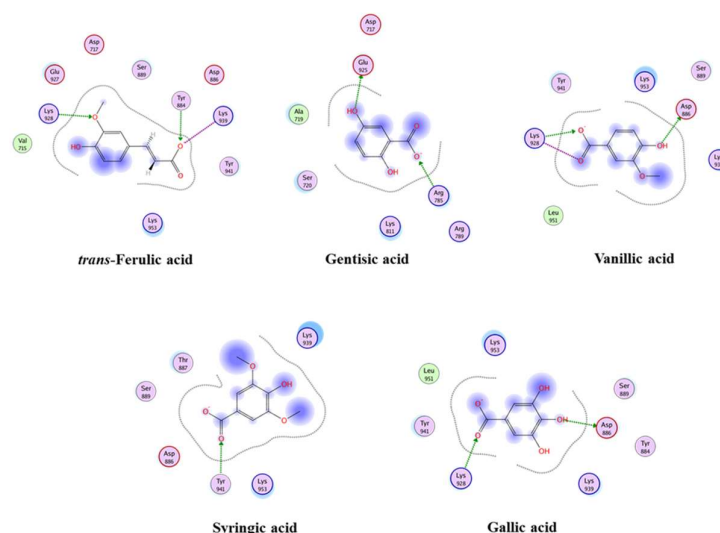

Figure 4. Fitting of phenolic acids in the DNA polymerase pocket.

There are two possible sites of association of amino acids to PA by hydrogen bonding - to the carboxyl group (protonated amino acids) or to the hydroxyl groups (neutral amino acids). The protonated amino acid takes part in hydrogen bonding by –NH3+ group, while the neutral amino acid by =O (-OH) groups. The complexes formed between hydroxybenzoic acids and the corresponding amino acids are shown in Fig. 7.
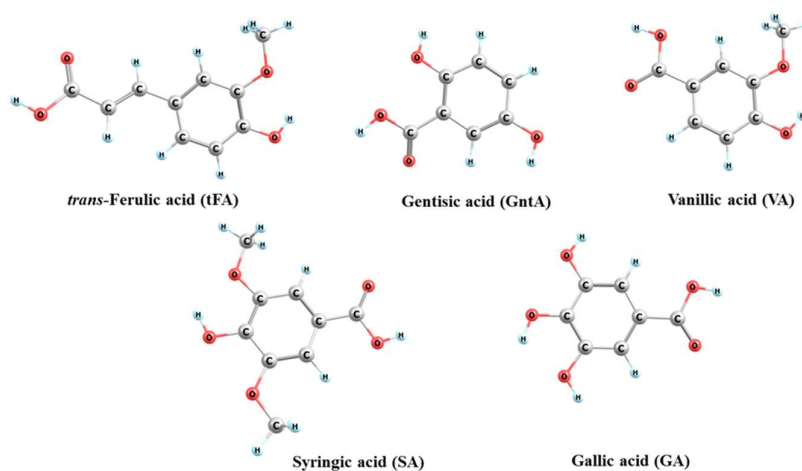

Figure 5. Structures of hydroxybenzoic acids from GP phenolic fraction "C", optimized at B3LYP/6-31+G(d,p) level.

To evaluate the binding expedient of PA to the corresponding AA of the enzyme active site and to compare it with a reference, quantum-chemical calculations on acyclovir triphosphate-amino acids complex were performed at the same theoretical level. This is necessary because the available treatments are based on several selective

drugs such as acyclovir, which are able to inhibit DNA polymerase [2]. In this way, the inhibitory activity of phenolic acids from GP to viral DNApol could be compared with that of acyclovir triphosphate (AcvTP). The surroundings in the active enzyme pocket of AcvTP were simulated similarly to phenolic acids, according to molecular docking results. The three hydroxyl groups from the phosphate residue in the acyclovir triphosphate molecule are deprotonated and interact with three protonated lysine molecules (at amino groups) in the enzyme active site (Fig. 8). AcvTP binds by hydrogen bonds to Glu, Tyr and two water molecules forming AcvTP-3pLys-Glu-Tyr-$2H_2O$ complex.

All species (PA, AcvTP, AA and water molecules), as well as all complexes, were optimized at the B3LYP/6-31+G(d,p) level of theory.

In order to evaluate the possibility of intermolecular hydrogen bonds formation between PA and AA, the energies of interaction (E_{int}) and interaction free Gibbs energies (G_{int}) were calculated by eq. (1) and (2):

$$E_{int} = E_{PA} + E_{AA} + 2E_{water} - E_{complex} \qquad (1)$$

$$G_{int} = G_{PA} + G_{AA} + 2G_{water} - G_{complex} \qquad (2)$$

E_{PA}, E_{AA}, $E_{water,}$ and $E_{complex}$ are the E_t energies; G_{PA}, G_{AA}, $2G_{water}$, and $G_{complex}$ are the G_{298} energies, calculated at B3LYP/6-31+G(d,p) level, for each phenolic acid, amino acids, AcvTP, water molecules and its complex, respectively. E_{int} and G_{298} of all complexes are presented in Table 2.

Table 2. Interaction energies, E_{int}, and interaction free Gibbs energies, G_{int}, (in kcal mol^{-1}), for the complexes of the GP hydroxybenzoic acids and acyclovir triphosphate (as a referent) with DNA polymerase amino acids calculated at B3LYP/6-31+G(d,p) and SMD/B3LYP/6-31+G(d,p) levels.

Complex type	E_{int}	G_{int}
gas phase		
*t*Fa-Lys-pTyr-Lys-$2H_2O$	163.40	104.12
GntA-Glu-pArg-$2H_2O$	163.63	119.89
VA-pLys-Asp-$2H_2O$	157.61	112.54
SA-pTyr-$2H_2O$	139.47	105.96
GA-Lys-pAsp-$2H_2O$	155.93	110.10
AcvTP-3pLys-Glu-Tyr-$2H_2O$	698.31	477.28
argon		
*t*Fa-Lys-Tyr-Lys-$2H_2O$	127.57	69.21
GntA-Glu-Arg-$2H_2O$	125.27	79.03
VA-Lys-Asp-$2H_2O$	119.93	76.36
SA-Tyr-$2H_2O$	106.23	71.37
GA-Lys-Asp-$2H_2O$	118.47	72.46
AcvTP-3Lys-Glu-Tyr-$2H_2O$	422.04	327.06

When the calculations were performed in gas phase, the most stable complex is that of AcvTP: AcvTP-3Lys-Glu-Tyr-$2H_2O$. The interaction energy (E_{int}) is 698.31 kcal mol^{-1}. According to our results for all phenolic acids, the most stable complexes are formed with *t*FA and GntA. The values of E_{int} are 163.40 and 163.63 kcal mol^{-1}, respectively. Next in the stability scale are the complexes of VA (157.61 kcal mol^{-1}) and GA (155.93 kcal mol^{-1}). As can be seen from the results received, the interaction energy of acyclovir triphosphate complex is more than four times higher than that of *t*FA and GntA

complexes (with highest E_{int}). The reason could be in the larger number of deprotonated -OH groups in the AcvTP molecule than in the phenolic acids ones. This leads to stronger binding of AcvTP to the active site of the enzyme compared to PA from GP.
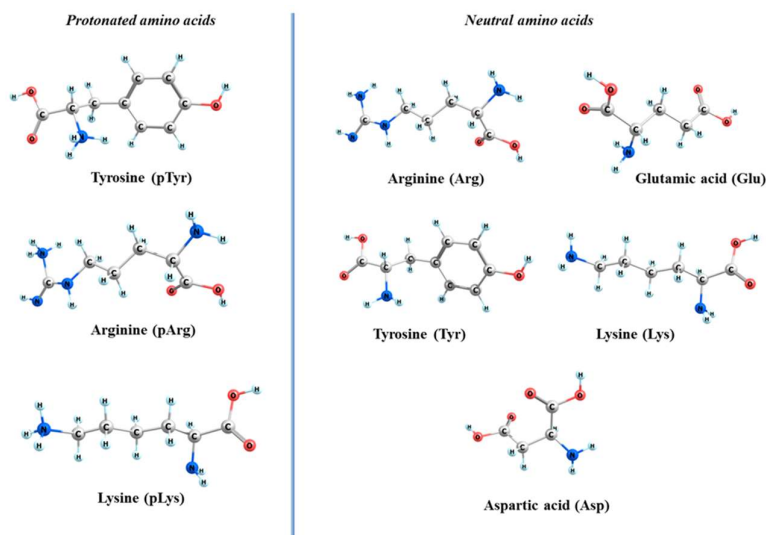

Figure 6. Structures of amino acids from GP phenolic fraction "C", optimized at B3LYP/6-31+G(d,p) level.

The picture is slightly different when the free Gibbs energies of interaction were considered: the AcvTP complex again has the highest interaction energy (477.28 kcal mol^{-1}), but the energy differences with hydroxybenzoic acids complexes decrease by an order of magnitude (Table 2). As can be seen from the table, all hydroxybenzoic acids complexes are close by free Gibbs interaction energy: between 104 and 119 kcal mol^{-1}.

When the SMD formalism at B3LYP/6-31+G(d,p) level was applied to account medium (argon) influence on the stability of the complexes formed, the energies of interaction E_{int} decrease drastically: by 276.27 kcal mol^{-1} for AcvTP complex and between 33-38 kcal mol^{-1} for the five phenolic acids complexes. In this case, *t*Fa-Lys-pTyr-Lys-$2H_2O$ and GntA-Glu-pArg-$2H_2O$ again show the greatest affinity for hydrogen bonding to the DNApol active site, compared to the complexes of other phenolic acids: 127.57 and 125.27 kcal mol^{-1}, respectively. If we consider the complexes of AcvTP and phenolic acids as embedded in a solvation model density, the SMD/B3LYP/6-31+G(d,p) calculated free interaction energies (G_{298}) decrease also: by 150.22 kcal mol^{-1} for AcvTP-3pLys-Glu-Tyr-$2H_2O$ and by 34-40 kcal mol^{-1} for hydroxybenzoic acids complexes, relative to the gas-phase cluster.

As can be seen from the results presented, compounds from the phenolic fraction of GP show the good possibility for hydrogen binding to DNApol active site but significantly smaller than that of AcvTp. This could be due to two facts: i) Methods based on functional density theory (DFT) provide treatment of the weak non-covalent interactions by false and irregular results. This is due to the fact that stabilization in these complexes is determined by dispersion interactions that are not accounted for by standard DFT functionalities [23]; ii). Despite the good results for the binding expedient of the phenolic fraction of GP, it is likely that the mechanism of action of these compounds includes inhibition of HSV-1 replication not only through DNA polymerase but probably by other enzymes. It is possible that the manner of the inhibitory activity on virus replication of AcvTP (by DNA polymerase) is different from that of the plant hydroxybenzoic acids one. Further investigations in this direction would help to clarify the antiviral activity of *Graptopetalum paraguayense* E. Walther.
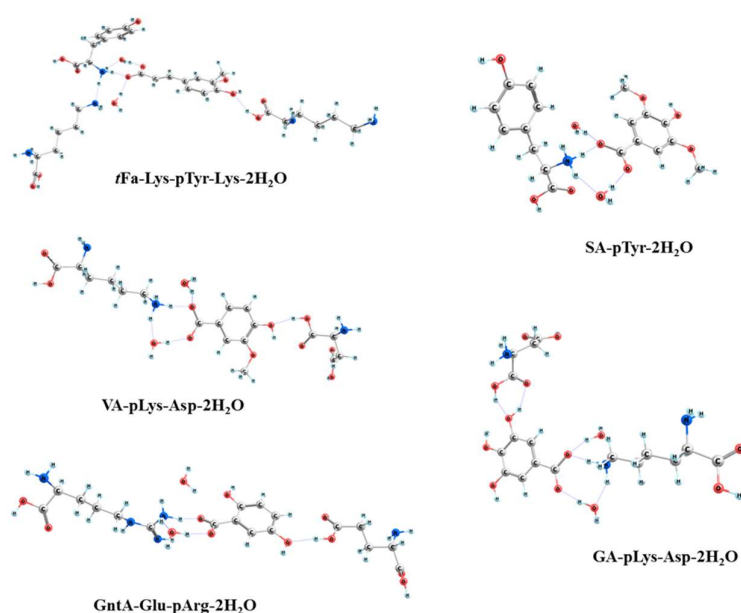
Figure 7. Complexes of phenolic acids from GP phenolic fraction "C" and amino acids from DNA polymerase active site, optimized at B3LYP/6-31+G(d,p) level.
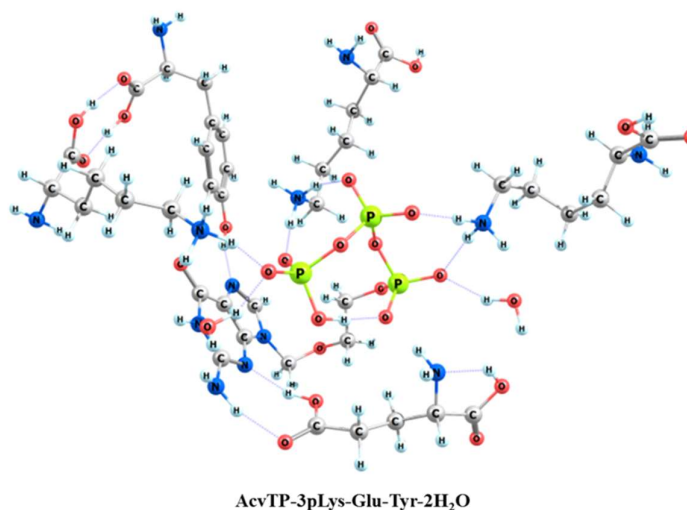

Figure 8. Complex of acyclovir triphosphate and amino acids from DNA polymerase active site, optimized at B3LYP/6-31+G(d,p) level.

4. Materials and Methods

4.1. Plant material and GP extracts preparation

4.1.1. Plant material

G. Paraguayense E. Walter was grown as an ornamental plant at the Institute of Organic Chemistry with Centre of Phytochemistry, Sofia, Bulgaria. Botanical identification and authentication were performed by Asen Asenov PhD (Sofia University 'St. Kliment Ohridski') and Antoaneta Petrova PhD (Botanical Garden, Bulgarian Academy of Sciences), and a voucher specimen number SO 107 621 was deposited in the herbarium of Sofia University, Bulgaria.

4.1.2. Chemicals

MeOH, CHCl$_3$, H$_2$SO$_4$, HCl, EtOAc, n-Hexane, Pyridine were HPLC grade (Sigma-Aldrich, St. Louis, MO). NaOH, Methoxyamine hydrochloride, BSTFA, nonadecanoic acid methyl ester, ribitol and 3-5-dichloro-4-methoxybenzoic acid were purchased from Sigma-Aldrich, St. Louis, MO and water was of Milli-Q (18 MΩ/cm) (Millipore Corp., Bedford, MA).

4.1.3. Extract preparation

Leaf extract was prepared as described in our previous study [22]. Briefly, 1.0 g of the freeze-dried material was mixed with 20.0 mL a methanol/water (75:25, v/v) solution and internal standards (nonadecanoic acid methyl ester, ribitol, and 3-5-dichloro-4-methoxybenzoic acid, each in concentration mg/mL for the quantification of metabolites of fractions A, B, and C, respectively), followed by heating at 70 °C for 1 h in a laboratory thermo mixer (Analytik Jena AG). The solution, cooling to room temperature was subjected to the following procedure: 8.0 mL chloroform and 2.0 mL water were added, then the mixture was centrifuged (5 min/22 °C/13000 rpm). The lower phase "A" was designed for the analysis of non-polar substances. The upper phase was divided into two equal parts (the first one "B" - for the study of the polar metabolites and the second one "C"- for the phenolic compounds). The three phases obtained were vacuum-dried in a centrifugal vacuum concentrator (Labconco Centrivap) at 40 ºC. To the dried residue of fraction "A" 1.0 mL 2% H$_2$SO$_4$ in methanol were added and the mixture was heated on Thermo-Shaker TS-100 (1 h/96 ºC/300 rpm). After cooling, the solution was extracted with n-hexane (3x10.0 mL). Combined organic layers were vacuum-dried in a centrifugal vacuum concentrator (Labconco Centrivap) at 40 ºC.

Fraction "C" was further processed. To the dried residue, 10.0 mL 1M NaOH (Sigma-Aldrich, MO) were added and the solution was kept overnight (12 h) at room temperature, then the pH was adjusted to 2 with 1M HCl and the mixture was heated on Thermo-Shaker TS-100 (1 h/96 ºC/300 rpm). After cooling, the solution was extracted with ethyl acetate (3x10.0 mL). Combined organic layers were vacuum-dried in a centrifugal vacuum concentrator (Labconco Centrivap) at 40 ºC. Fractions "A", "B" and "C" were subjected to further analyses.

4.1.4. GC-MS sample preparation

Prior to the GC-MS analysis, fractions "A", "B" and "C" were derivatized by the following procedures. 100.0 µL pyridine and 100.0 µL N,O-Bis(trimethylsilyl)trifluoroacetamide (BSTFA) were added to the dried residues (fractions "A" and "C"), then heated on Thermoshaker, Analytik Jena AG, Germany (45 min/70ºC/300 rpm). 1.0 µL from the solution was injected into the GC-MS.

300.0 µL solution of methoxyamine hydrochloride (20.0 mg/mL in pyridine) was added to 5.0 mg fraction "B", and the mixture was heated on Thermo-Shaker TS-100 (1h/70ºC/300 rpm). After cooling, 100.0 µL N,O-Bis(trimethylsilyl)trifluoroacetamide (BSTFA) were added to the mixture, then heated on Thermoshaker, Analytik Jena AG, Germany (40 min/70 ºC/300 rpm). 1.0 µL from the solution was injected into the GC-MS.

4.1.5. GC-MS

GC-MS analysis was carried out on a 7890A gas chromatograph (Agilent Technologies) interfaced with a 5975C mass selective detector (Agilent Technologies). Separations were performed using a 30m x 0.25 mm (i.d.) DB-5ms silica-fused capillary column coated with 0.25 µm film of poly (dimethylsiloxane) as the stationary phase. The flow rate of the carrier gas (helium) was maintained at 1.0 ml/min. The injector and the transfer line temperature were kept at 250 °C. The oven temperature program used was: 100°C for 2 min then 15 °C/min to 180 °C for 1min then 5 °C/min to 300 °C for 10 min. The injections were carried out in a split mode (10:1). The mass spectrometer was scanned from 50 to 550 m/z. All mass spectra were acquired in electron impact (EI) mode with 70 eV.

A mixture of aliphatic hydrocarbons (C8-C40) (Sigma) was injected into the system under the above temperature program in order to calculate the retention index RI (as Kovàts index) of each compound. Identification of compounds was obtained by comparing the RI and the spectral data from the Golm Metabolome Database (http://csbdb.mpimp-golm.mpg.de/csbdb/gmd/gmd.html) and NIST'08 (National Institute of Standards and Technology, USA).

4.2. Computational details
4.2.1. Molecular docking analysis

Fourteen different phenolic acids such as gallic, *trans*-ferulic, syringic acids, and others found by GS-MS analyses, were used in molecular docking simulations. For our model, we used the structure with PDB number 2GV9, which is a structure of the Herpes Simplex virus type 1 DNA polymerase, obtained by XRD with an overall resolution of 2.68 Å [24]. The crystal structure was a dimer and for further work, we selected the B chain as it has fewer missing amino acids. The protein structure was prepared for docking according to the implemented structure preparation algorithm in MOE software [25] and was protonated according to the implemented Protonate3D algorithm. The resultant structure was relaxed by rough steepest descent optimization with MMFF94 force field and Born solvation water model. The site finder algorithm [25] was used to identify sites for the docking procedure and two of them, that lie on the contact surface between protein and DNA and are close to amino acids in active site of the DNA polymerase, were selected for further work. Conformation library for the docking study was generated using LowModeMD methodology with MMFF94 force field and energy window for collection of conformations 50 kcal mol^{-1} from the lowest energy conformation. All conformations of all ligands were docked in the two selected pockets using Triangle Matcher algorithm for the initial placement of every structure, which returns up to 10 000 000 poses of every ligand inside a pocket. These poses were scored by London ΔG [25] function, which estimates the free energy of binding of the ligand from a given pose and consists of terms that weigh up average gain/loss of rotational and translational entropy and loss of flexibility of the ligand, measures geometric imperfections of hydrogen bonds and desolvation energy of atoms.

The best 50 poses for every ligand for every pocket were further optimized with Induced Fit methodology using MMFF94 force field and optimization cutoff of 6A from the ligand [26]. The GBVI/WSA ΔG [25] was used as a rescoring function and the best 30 poses were collected for the next coming analysis.

4.2.2. Quantum-chemical calculations

According to the interaction energies of all fourteen ligands (phenolic acids from fraction "C") in the pockets based on the GBVI/WSA ΔG scoring function, DFT calculations were performed on the five optimally interacting with the receptor acids. The B3LYP [27, 28] functional has been widely used over the years as it has been found to provide a good balance between speed and accuracy. Thus, geometric optimization of the hydroxybenzoic acids *trans*-ferulic, gallic, syringic, vanillic, gentisic acids, and acyclovir, as well as amino acids from DNA polymerase active site and the complexes of the phenolic acids (and acyclovir) with amino acids, was carried out at B3LYP/6-31+G(d,p) computational level without symmetry constraints. Hydroxybenzoic acids and some of the amino acids that interact in the active center pocket of the enzyme are deprotonated. The same applies to acyclovir and its interacting amino acids. Acyclovir as an inhibitor of viral DNA synthesis is monophosphorylated by virus-encoded thymidine kinase (TK). Subsequent diphosphorylation and triphosphorylation are catalyzed by host cell enzymes, resulting in acyclovir triphosphate [29]. Therefore, we use in our model acyclovir triphosphate (deprotonated at the three hydroxyl groups) located in the active site of HSV DNA polymerase. The local minima were verified by establishing that the Hessians had zero eigenvalues. The values of Gibbs free energies

(G_{298}) were calculated for a temperature of 298.15 K. To simulate the medium influence, the structures of acyclovir triphosphate, phenolic and amino acids as well as their complexes, were optimized again in argon medium (ε=1.430) using solvation model density (SMD) of Truhlar and coworkers [30] at the same computational level (SMD/B3LYP/6-31+G(d,p)). This is the recommended choice for computing ΔG of solvation and it has the advantage of being parameterized for more than 100 solvents. The dielectric constant of the medium (the pocket of the enzyme site surrounding the phenolic acid and acyclovir complexes) was set to 1 and we chose the argon as medium to mimic the nature of the enzyme inside based on the previous studies [31, 32]. The nature of the local minima on the potential energy surface was checked again by the absence of imaginary frequency. The DFT calculations were performed using Gaussian09 software package [33].

5. Conclusions

Current treatment for HSV infection relies mainly on the use of acyclovir and related synthetic nucleoside analogs. The widespread use of these drugs has led to the establishment of side effects and drug-resistant strains, which has increased the need for new natural antiviral agents. Total methanol extract from the succulent plant *Graptopetalum paraguayense* E. Walther demonstrates a significant inhibitory effect on HSV-1, according to our recent study [22]. In order to explain this strong antiviral activity, metabolic analysis of the plant was performed. Three main fractions: non-polar substances, polar metabolites, and phenolic compounds were obtained and GC-MS analysis was carried out. Fourteen different phenolic acids such as gallic, *trans*-ferulic, syringic acids, and others found by GS-MS analyses, were used in molecular docking simulations. The optimally interacting with the receptor amino acids were used for quantum-chemical calculations at B3LYP/6-31+G(d,p) computational level to establish the binding affinity of hydroxybenzoic acids from GP to HSV DNApol active site. According to the interaction energies of all five ligand-amino acid complexes, the hydrogen bonding in all of them is strong but significantly weaker than that in the acyclovir complex. The reason could be in DFT methods used as well as in the mechanism of antiviral effect. It is possible the mode of the inhibitory activity on the virus replication of AcvTP (by DNA polymerase) is different from that of the plant hydroxybenzoic acids one. Further investigations in this sense would help to clarify the antiviral activity of *Graptopetalum paraguayense* E. Walther.

References

1. Boppana, S. B.; Fowler, K. B., Persistence in the population: epidemiology and transmisson. In *Human Herpesviruses: Biology, Therapy, and Immunoprophylaxis*, Arvin, A.; Campadelli-Fiume, G.; Mocarski, E.; al., e., Eds. Cambridge University Press: Cambridge, 2007.

2. Denaro, M.; Smeriglio, A., Antiviral activity of plants and their isolated bioactive compounds: An update. *Phytother Res* **2020,** 34, (4), 742-768.

3. Naray-Szabo, G., Quantum chemical calculation of the enzyme-ligand interaction energy for trypsin inhibition by benzamidines. *J Am Chem Soc* **1984,** 106, (16), 4584-4589.

4. Himo, F., Recent Trends in Quantum Chemical Modeling of Enzymatic Reactions. *J Am Chem Soc* **2017,** 139, (20), 6780-6786.

5. Perez, R. M., Antiviral Activity of Compounds Isolated From Plants. *Pharm. Biol.* **2003,** 41, (2), 107-157.

6. Treml, J.; Gazdová, M.; Šmejkal, K.; Šudomová, M.; Kubatka, P.; Hassan, S. T. S., Natural Products-Derived Chemicals: Breaking Barriers to Novel Anti-HSV Drug Development. *Viruses* **2020,** 12, (2), 154.

7. Hassan, S. T. S.; Masarčíková, R.; Berchová, K., Bioactive natural products with anti-herpes simplex virus properties. *J Pharm Pharmacol* **2015,** 67, (10), 1325-1336.

8. Saxena, M.; Saxena, D. J.; Pradhan, D. A., Flavonoids and phenolic acids as antioxidants in plants and human health. *J. Pharm. Sci. Rev. Res.* **2012,** 16, (2), 130-134.

9. Medini, F.; Megdiche, W.; Mshvildadze, V.; Pichette, A.; Legault, J.; St-Gelais, A.; Ksouri, R., Antiviral-guided fractionation and isolation of phenolic compounds from Limonium densiflorum hydroalcoholic extract. *C. R. Chim.* **2016,** 19, (6), 726-732.

10. Suárez, B.; Álvarez, Á. L.; García, Y. D.; Barrio, G. d.; Lobo, A. P.; Parra, F., Phenolic profiles, antioxidant activity and in vitro antiviral properties of apple pomace. *Food Chem* **2010,** 120, 339-342.

11. Reichling, J.; Neuner, A.; Sharaf, M.; Harkenthal, M.; Schnitzler, P., Antiviral activity of *Rhus aromatica* (fragrant sumac) extract against two types of herpes simplex viruses in cell culture. *Die Pharmazie* **2009,** 64, (8), 538-41.

12. Nolkemper, S.; Reichling, J.; Sensch, K. H.; Schnitzler, P., Mechanism of herpes simplex virus type 2 suppression by propolis extracts. *Phytomedicine* **2010,** 17, (2), 132-8.

13. Huang, K. F.; Chen, Y. W.; Chang, C. T.; Chou, S. T., Studies on the inhibitory effect of *Graptopetalum paraguayense* E. Walther extracts on mushroom tyrosinase. *Food Chem* **2005,** 89, (4), 583-587.

14. Chao, W. W.; Chen, S. J.; Peng, H. C.; Liao, J. W., Antioxidant Activity of *Graptopetalum paraguayense* E. Walther Leaf Extract Counteracts Oxidative Stress Induced by Ethanol and Carbon Tetrachloride Co-Induced Hepatotoxicity in Rats. *Antioxidants (Basel, Switzerland)* **2019,** 8, (8), 251-265.

15. Chen, S. J.; Chang, C. T.; Chung, Y. C.; Chou, S. T., Studies on the inhibitory effect of *Graptopetalum paraguayense* E. Walther extracts on the angiotensin converting enzyme. *Food Chem* **2007,** 100, 1032–1036.

16. Chung, Y.-C.; Chen, S.-J.; Peng, H.-Y.; Chou, S.-T., Antihypertensive and antioxidant effects of the *Graptopetalum paraguayense* E. Walther extract in spontaneously hypertensive rats. *J Sci Food Agric.* **2009,** 89, (15), 2678-2686.

17. Duh, P.-D.; Lin, S.-L.; Wu, S.-C., Hepatoprotection of *Graptopetalum paraguayense* E. Walther on CCl4-induced liver damage and inflammatio. *J Ethnopharmacol* **2011,** 134, 379–385.

18. Hsu, W. H.; Liao, S. C.; Chyan, Y. J.; Huang, K. W.; Hsu, S. L.; Chen, Y. C.; Siu, M. L.; Chang, C. C.; Chung, Y. S.; Huang, C. F., *Graptopetalum paraguayense* Inhibits Liver Fibrosis by Blocking TGF-beta Signaling In Vivo and In Vitro. *Int J Mol Sci* **2019,** 20, (10), 2592.

19. Ai, L.; Chung, Y.-C.; Jeng, K.-C. G.; Lai, P. F. H.; Yeh, S.-C.; Lee, K. C.; Lin, S.-Y.; Xia, Y.; Wang, G.; Cui, S. W., Antioxidant hydrocolloids from herb *Graptopetalum paraguayense* leaves show anti-colon cancer cells and anti-neuroinflammatory potentials. *Food Hydrocoll.* **2017,** 73, 51-59.

20. Chen, S.-J.; Yen, C.-H.; Liu, J.-T.; Tseng, Y.-F.; Lin, P.-T., Anti-inflammatory effect of water extracts of *Graptopetalum paraguayense* supplementation in subjects with metabolic syndrome: a preliminary study. *J Sci Food Agric* **2016,** 96, (5), 1772-1776.

21. Wu, P.-C.; Fann, M.-J.; Tran, T. T.; Chen, S.-C.; Devina, T.; Cheng, I. H.-J.; Lien, C.-C.; Kao, L.-S.; Wang, S.-J.; Fuh, J.-L.; Tzeng, T.-T.; Huang, C.-Y.; Shiao, Y.-J.; Wong, Y.-H., Assessing the therapeutic potential of *Graptopetalum paraguayense* on Alzheimer's disease using patient iPSC-derived neurons. *Sci Rep* **2019,** 9, (1), 19301.

22. Zaharieva, M. M.; Genova-Kalou, P.; Dincheva, I.; Badjakov, I.; Krumova, S.; Enchev, V.; Najdenski, H.; Markova, N., Anti-Herpes Simplex virus and antibacterial activities of *Graptopetalum paraguayense* E. Walther leaf extract: a pilot study. *Biotechnol Biotechnol Equip* **2019,** 33, (1), 1251-1259.

23. Rajchel, Ł.; Żuchowski, P. S.; Hapka, M.; Modrzejewski, M.; Szczęśniak, M. M.; Chałasiński, G., A density functional theory approach to noncovalent interactions via interacting monomer densities. *Phys chem chem phys* **2010,** 12, (44), 14686-14692.

24.   Liu, S.; Knafels, J. D.; Chang, J. S.; Waszak, G. A.; Baldwin, E. T.; Deibel, M. R., Jr.; Thomsen, D. R.; Homa, F. L.; Wells, P. A.; Tory, M. C.; Poorman, R. A.; Gao, H.; Qiu, X.; Seddon, A. P., Crystal structure of the herpes simplex virus 1 DNA polymerase. *J. Biol. Chem* **2006,** 281, (26), 18193-200.

25.   Group, C. C. *MOE – MOE Software package* QC: Montreal, Canada, 2020.

26.   Naïm, M.; Bhat, S.; Rankin, K. N.; Dennis, S.; Chowdhury, S. F.; Siddiqi, I.; Drabik, P.; Sulea, T.; Bayly, C. I.; Jakalian, A.; Purisima, E. O., Solvated Interaction Energy (SIE) for Scoring Protein–Ligand Binding Affinities. 1. Exploring the Parameter Space. *J Chem Inf Model* **2007,** 47, (1), 122-133.

27.   Becke, A. D., Density-functional thermochemistry. III. The role of exact exchange. *J. Chem. Phys.* **1993,** 98, (7), 5648-5652.

28.   Lee, C. T.; Wang, W. T.; Pople, R. G., Development of the Colle-Salvetti correlation-energy formula into a functional of the electron density. *Phys. Rev. B* **1988,** 37, 785-789.

29.   Kimberlin, D. W., 295 - Antiviral Agents. In *Principles and Practice of Pediatric Infectious Diseases (Fifth Edition)*, Long, S. S.; Prober, C. G.; Fischer, M., Eds. Elsevier: 2018; pp 1551-1567.e6.

30.   Marenich, A. V.; Cramer, C. J.; Truhlar, D. G., Universal solvation model based on solute electron density and on a continuum model of the solvent defined by the bulk dielectric constant and atomic surface tensions. *J. Phys. Chem. B* **2009,** 113, 6378.

31.   Foley, M. C.; Padow, V. A.; Schlick, T., DNApol λ's extraordinary ability to stabilize misaligned DNA. *J Am Chem Soc* **2010,** 132, (38), 13403-16.

32.   Ceña-Diez, R.; Vacas-Córdoba, E.; García-Broncano, P.; de la Mata, F. J.; Gómez, R.; Maly, M.; Muñoz-Fernández, M., Prevention of vaginal and rectal herpes simplex virus type 2 transmission in mice: mechanism of antiviral action. *Int. J. Nanomed* **2016,** 11, 2147-62.

33.   Frisch, M. J.; Trucks, G. W.; Schlegel, H. B.; Scuseria, G. E.; Robb, M. A.; Cheeseman, J. R.; Scalmani, G.; Barone, V.; Mennucci, B.; Petersson, G. A.; Nakatsuji, H.; Caricato, M.; Li, X.; Hratchian, H. P.; Izmaylov, A. F.; Bloino, J.; Zheng, G.; Sonnenberg, J. L.; Hada, M.; Ehara, M.; Toyota, K.; Fukuda, R.; Hasegawa, J.; Ishida, M.; Nakajima, T.; Honda, Y.; Kitao, O.; Nakai, H.; Vreven, T.; Montgomery, J. A., Jr.; Peralta, J. E.; Ogliaro, F.; Bearpark, M.; Heyd, J. J.; Brothers, E.; Kudin, K. N.; Staroverov, V. N.; Kobayashi, R.; Normand, J.; Raghavachari, K.; Rendell, A.; Burant, J. C.; Iyengar, S. S.; Tomasi, J.; Cossi, M.; Rega, N.; Millam, J. M.; Klene, M.; Knox, J. E.; Cross, J. B.; Bakken, V.; Adamo, C.; Jaramillo, J.; Gomperts, R.; Stratmann, R. E.; Yazyev, O.; Austin, A. J.; Cammi, R.; Pomelli, C.; Ochterski, J. W.; Martin, R. L.; Morokuma, K.; Zakrzewski, V. G.; Voth, G. A.; Salvador, P.; Dannenberg, J. J.; Dapprich, S.; Daniels, A. D.; Farkas, Ö.; Foresman, J. B.; Ortiz, J. V.; Cioslowski, J.; Fox, D. J. *Gaussian 09, Revision D.01*, Wallingford CT: 2009.